Worldwide Oceanic Wind and Wave Predictions Using a Satellite Radar-Radiometer

RICHARD K. MOORE*
The University of Kansas, Lawrence, Kan.

AND

WILLARD J. PIERSON JR.†
New York University, Bronx, N.Y.

Data from a combined radar-radiometer in a satellite should permit improved prediction of surface atmospheric pressure, winds, and ocean wave spectra on a global basis, with consequent advantages to shipping. Radar returns from the sea at 2.25-cm wavelength have been measured and shown to be proportioned to windspeed. Use of a microwave radiometer should permit removing false radar data caused by atmospheric attenuation since the radiometric temperature is highly sensitive to such attenuation.

A Proposed Satellite Instrument

PREDICTION of ocean wave spectra involves knowledge of the surface wind field over a large area and a long time. Since ocean waves can propagate great distances, and the effect of local winds is felt for many hours after the winds have died down, numerical prediction techniques depend on iterative solution of the appropriate equations over the period of about a week using both past observed winds and forecasted winds. Updating at 24-hr intervals permits the predictions to be continuously extended. The grid for numerical forecasting is that of the synoptic scale and accordingly a 120-km point spacing is used. This permits the satellite instrument to operate with a resolution of tens of kilometers, which greatly simplifies its design.

Instruments on NASA aircraft flying over the North Atlantic in March of 1968 and 1969 determined the dependence of the radar scattering coefficient at 2.25-cm wavelength on windspeed. Similar observations (1969 only) indicate that a 75-cm wavelength is unsuitable for sea-surface wind determination.

A scanning radar-radiometer, proposed as a spacecraft instrument, will operate its radar in an ICW (interrupted continuous wave) mode. Radiometer and radar can use the same receiver, except that the bandwidth of the radar must at some point be narrowed to that of the Doppler frequency spread of the returns. Because the radiometer output is sensitive to the clouds and rain that cause heavy radar attenuation, the radiometer signal can be used to calibrate the radar.

Observations from several orbits of this instrument must be integrated with cloud pictures and surface observations to obtain an analysis of the winds and pressures over the oceans. The direction of the wind being measured by the radar must be obtained from other observations since the radar only gives speed. Southern hemisphere analyses and predictions will be greatly improved because conventional surface observations are scarce.

Radar Observations of Ocean Backscatter

Many of the measurements of backscatter of radar waves from the sea, made since early in World War II, are summarized in Beckmann and Spizzichino[1] and in Skolnik.[2] Unfortunately, however, most such observations were made at nearly grazing angles of incidence, or suffered from lack of information about the surface of the sea, or were made near coasts. Apparently, measurements have been made over the open sea during high-wind conditions and at angles of incidence in the middle range[3,4] only within the last two years.

From the early observations to the present, off-vertical backscatter has apparently increased with increasing "sea state." Attempts have been made to relate this phenomenon to both wave height and windspeed; but in recent years it has become apparent that windspeed is more important than wave height in determining radar return, at least for most angles of incidence and for microwavelengths. This is probably due to the strong dependence of the radar return on the high-wavenumber part of the ocean wave spectrum (i.e., the small structure), and the dependence in turn of this part of the wave structure on the current local wind.[5–7]

Various observers have indicated some sort of saturation in the increase of radar return with windspeed,[4,8] and Wright[5] has predicted this saturation on the basis of a perturbation theory for radar scatter and the Phillips expression for the high-frequency tail of the ocean wave spectrum. The validity of this prediction and of the observations of saturation seems to be dependent on radar wavelength and on the approximations both in the radar theory and in the use of the Phillips spectral form. Evidence reported here indicates no saturation for 2.25-cm radar wavelength up to windspeeds between 40 and 50 knots, whereas little change appears to be present for 75-cm radar waves. The NRL measurements[4] at 3.3 cm show a much smaller variation with windspeed than reported here at 2.25 cm, and the NRL measurements at longer wavelengths show almost no increase in radar return at mid-angles for windspeeds above about 12 knots.

A NASA/MSC aircraft operating in the Earth Resources Observation Program made flights over the North Atlantic in the spring of 1968 from a base at Keflavik, Iceland, and in the spring of 1969 from a base at Shannon, Ireland. Two radar scatterometers were carried on these missions, one at 2.25-cm radar wavelength (both missions) and the other at 75-cm radar wavelength (1969 mission only). During the 1969 mission, Nordberg of NASA-GSFC made essentially simultaneous radiometer measurements at 1.6 and 3.2 cm using a different aircraft.

The radar systems used for these measurements transmitted unmodulated carriers into fan beams along the aircraft flight track. Back-scatter from different angles of incidence was separated by filtering out returns that had undergone different Doppler-frequency shifts. That is, the frequency of the

Presented as Paper 70-310 at the AIAA Earth Resources Observations and Information Systems Meeting, Annapolis, Md., March 2–4, 1970; submitted March 11, 1970; revision received October 19, 1970.

* Black and Veatch Professor of Electrical Engineering, Center for Research in Engineering Science.

† Professor, Department of Meteorology and Oceanography.

return from each angle of incidence ahead of the aircraft was shifted up by a unique amount associated with the unique relative velocity in that direction between the aircraft and the sea; and the return from each angle of incidence behind the aircraft suffered a similar downward frequency shift. Use of narrow-band filters permitted isolation of returns from narrow ranges of incident angle.

Absolute calibration of the radar differential scattering coefficient measurements depends on monitoring the ratio of the transmitted-to-received power accurately, but relative measurement of the scattering coefficients at different angles of incidence depends only on the stability of the gain vs frequency characteristic of the receiver, on the stability (not accuracy) of the antenna gain, and on knowledge of the aircraft ground speed (obtained independently from a Doppler navigator). Observation of the results indicates that the calibration method used at 2.25 cm may cause errors in the absolute measurement as high as ±3 db, but the measurements were repeatable at most to ±1 db. At 75 cm the absolute measurements beyond 20° are considerably better than those at 2.25 cm, with exact accuracy as yet undetermined. Within 20° of vertical, the 75-cm measurements may be less accurate because of errors in relating aircraft attitude to antenna pattern. Beyond 35° the low signal-to-noise ratio makes the results questionable.

Because the relative measurements are much more accurate than the absolute measurements, the 2.25-cm observations have been normalized to 10°. Figure 1 shows the normalized 2.25-cm upwind measurements for a variety of windspeeds and for runs made during both years. The ordinate is the ratio of the differential scattering coefficient ($\sigma°$) at each angle to that at 10°, expressed in db. Clearly, the normalized value of $\sigma°$ increases with increasing windspeed for all angles above 10°. Figure 2 shows the difference between upwind and crosswind data. Not only are the crosswind values less, but their variation with windspeed is different from that for upwind data.

Although observation of Figs. 1 and 2 might lead to the conclusion that the variation with windspeed saturates, use of logarithmic scales for both windspeed and $\sigma°$ in Fig. 3 shows that the 35° scattering continues to increase up to the maximum windspeed for which observations are available.

From these results, use of radar cross section as a measure of windspeed appears feasible, provided the wind direction is known. On the basis of the relative measurements, a system that measures $\sigma°$ at two angles (say, 10° and 35°) along the satellite ground track can be justified. Both previous measurements and theory indicate that the curves of absolute

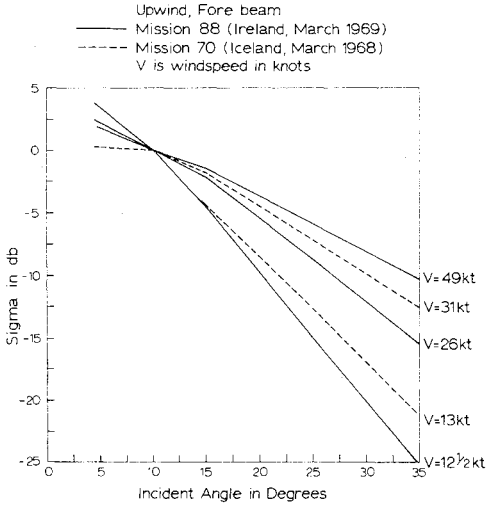

Fig. 1 Differential scattering coefficient of ocean at 2.25-cm wavelength normalized to 0 db at 10°.

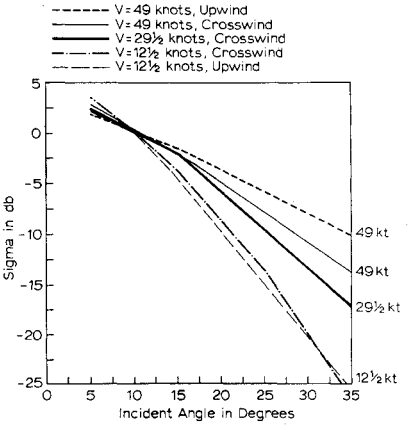

Fig. 2 Comparison of crosswind and upwind data, Mission 88 (Ireland, March 1969).

magnitude of the differential scattering coefficient should cross each other in the vicinity of 10°, as do the normalized curves. The system proposed here is based on this assumption.

The measurements at 75-cm wavelength show, if anything, a reverse trend with respect to windspeed, but this trend is small enough to be due to measurement error. Figure 4 compares the limits observed with representative data at 2.25 cm and 75 cm. Scatter at 75 cm may not show significant changes until the winds become quite high as the roughness elements correspond to longer gravity waves.

Guinard's[4] 3.3-cm measurements show the same trend as the 2.25-cm NASA results, but with much less sensitivity to windspeed. Thus, it appears that proper choice of wavelength for radar determination of windspeed is very important. Since no suitable data are available at somewhat shorter wavelengths, continuation of the increase in windspeed sensitivity with decreasing wavelength cannot be verified.

Microwave Radiometric Measurements of Sea and Precipitation

Although microwave radiometric observations of relatively calm seas and of controlled surfaces have been available for some time,[9] Nordberg[10] apparently made the first measurements of microwave brightness temperature of the ocean under high sea state conditions during 1969. The microwave radiometer aircraft was faster than the radar aircraft, so that it was possible to extend the measurements to a larger region with more variable conditions; but the best information about surface conditions was obtained at the same ships as used for the radar measurement.

When the microwave radiometers were carried over a wide range of sea conditions from less than 12-knot winds to 50-knot or greater winds, the measured effective temperature of the surface increased from about 105° to about 125° at 3.2-cm wavelength. Qualitative observations, when correlated with an experiment by Williams[11] using foam in a water tank, appear to show that much of the increase is due to an increase in the amount of foam on the ocean as the windspeed picks up, but this has not yet been fully verified. The increase in effective temperature was greater at 1.6 cm than at 3.2 cm.

Although this experiment showed that the microwave radiometer response is proportional to windspeed, the experiment also showed that a much greater effective temperature increase occurs when the radiometer flies over precipitation. Since precipitation is a cause of significant absorption of microwaves, and any absorber is also a radiator, this effect was to be expected.[12,13] If the absorption is sufficiently strong, the effective temperature seen by the antenna is essentially the actual temperature of the absorbing medium.

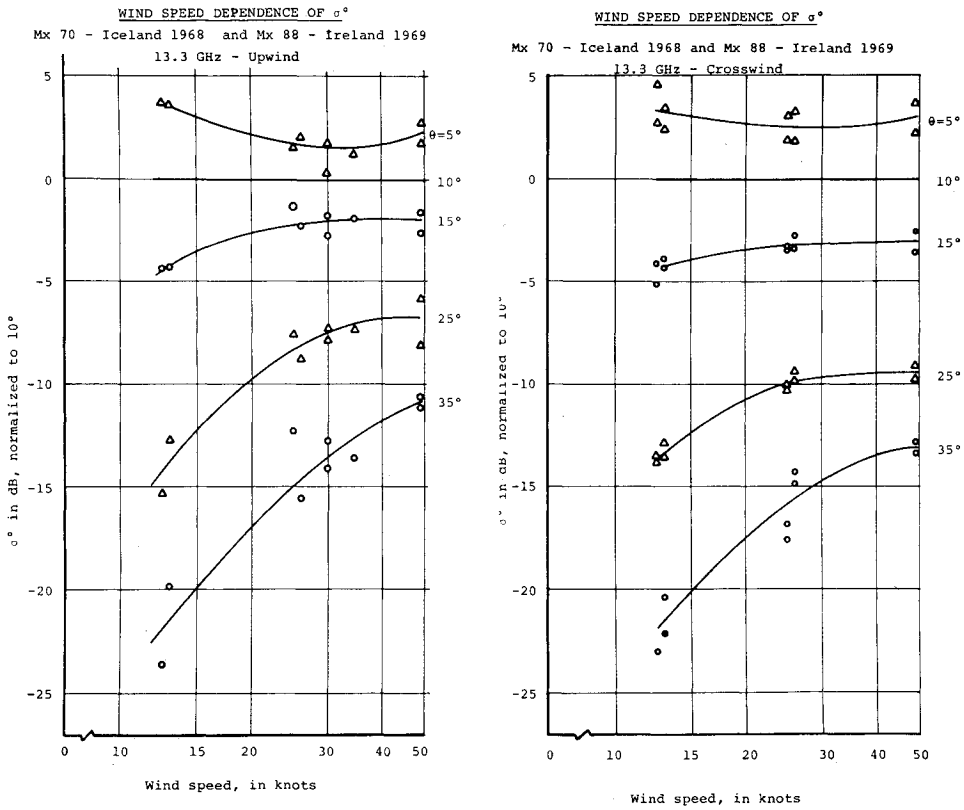

Fig. 3 Normalized radar scattering coefficient vs windspeed and direction at 13.3 GHz.

Since this temperature is always far above the effective temperature of the ocean surface, flying over a precipitating cloud causes large increases in the apparent temperature seen by the radiometer.

Although this increase in radiation from a precipitating cloud has been observed many times, the most significant measurements for our purpose relate the attenuation through the precipitation, or cloud, with the emission from it. Wilson[14] used an upward-looking radiometer to compare attenuation of microwave solar radiation with brightness temperature from the attenuating region; Figure 5 illustrates Wilson's findings that are relevant to this study. The agreement between attenuation computed on the basis of microwave emission from the precipitation and that measured for the solar radiation is excellent for attenuations less than about 10 db.

The accuracy of the calculations of attenuation based on measured microwave brightness depends on the stability of the model atmosphere used. The total emission is directly proportional to total absorption, but emission from the more distant parts of the atmosphere is attenuated itself, and the model must take this into account. Since Wilson's observations were in New Jersey, where most attenuation and radiation comes from rain, a different model is undoubtedly required in the wet tropics, where dense clouds may be a major source of attenuation and radiation. Furthermore, the model should account differently for absorption and scattering.

Measurements with both microwave radiometers and scatterometers[15] over sea ice show much stronger signals than those from the sea itself at the angles of incidence considered here. In regions where sea ice occurs, attenuation and emission in clouds and precipitation is small, so both a radiometer and a radar carried on a satellite will experience strong signal increases in going from sea to ice.

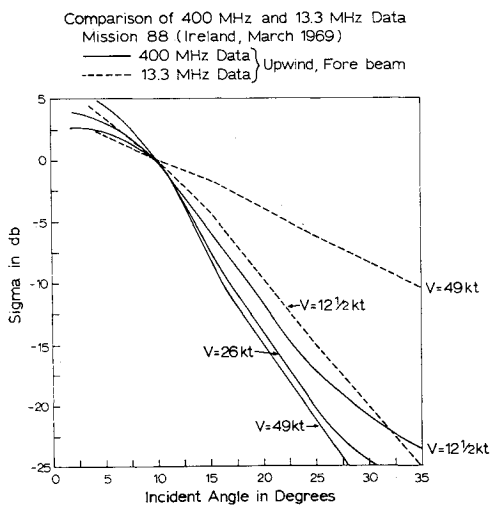

Fig. 4 Differential scattering coefficient of ocean, normalized to 0 db at 10°.

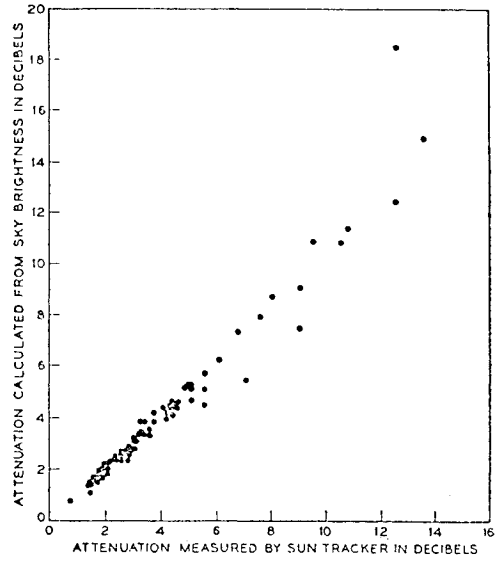

Fig. 5 Vertical caption: attenuation calculated from sky brightness in decibels. Horizontal caption: attenuation measured by sun tracker in decibels.

RADSCAT—A Satellite Radiometer-Scatterometer System

Since observations and theory indicate that radar return from the sea at centimeter wavelengths is a measure of the local winds, a satellite radar scatterometer should be able to map the surface wind fields over the oceans. On the other hand, attenuation by rain on the backscattered signal may be a problem for a centimeter-wavelength radar. Addition of a radiometer to the system will permit determining the attenuation to sufficient accuracy to correct the observed radar signals.

The same receiver, with two branches, can be used for both the radar and the radiometer. Thus, the radiometer-scatterometer contains the same elements as a radiometer alone, plus a transmitter and a narrow band filter for the radar part of the receiver.[16]

The Dicke radiometer[17] compares the received sum of signal and noise to the output of a calibrated noise source; a switch alternates the input and output of the receiver between the antenna and the noise calibration source. By integrating for a sufficient time, the mean value of each output is estimated with variance small enough so that the mean signal can be obtained accurately by subtracting the noise output from the sum output. The same technique is used for the radar in the proposed system. With the radiometer, noise-like signals as weak as 30 db below the receiver noise can be readily extracted. With the radar, however, the bandwidth of the noise-like signal is determined by the spread of Doppler frequencies between the forward and rear part of the illuminated ground area. This bandwidth is so narrow for the case at hand that too few independent samples are obtained to permit measurement of signals much smaller than the receiver noise. This concept is illustrated in Fig. 6.

In the RADSCAT system, the transmitter emits continuous sine waves until just before the first return from the sea is expected; at this time it is turned off. The returned signal lasts somewhat longer than that transmitted because of differences in range (and thus delay time) between the inner and outer edge of the illuminated patch of sea. During the reception period, the output of the receiver is channeled to the radar detector through a filter whose bandwidth is matched to that of the Doppler frequency spectrum of the incoming signal. After detection, this signal is integrated to reduce its variance.

When the radar signal ends, the output of the wide-bandwidth filter connects to the radiometer detector, with subsequent integration. This radiometer output also provides the noise calibration for the radar receiver, since noise for the radar includes both that due to the receiver and that due to atmospheric and surface emission received by the antenna. The radiometer reciever is provided with a signal from the calibration source, either during a subsequent interval or during the transmitting period.

In summary, the operation of the system involves four separate time intervals: radar transmission; radar reception; radiometer reception, which is also radar calibration; and

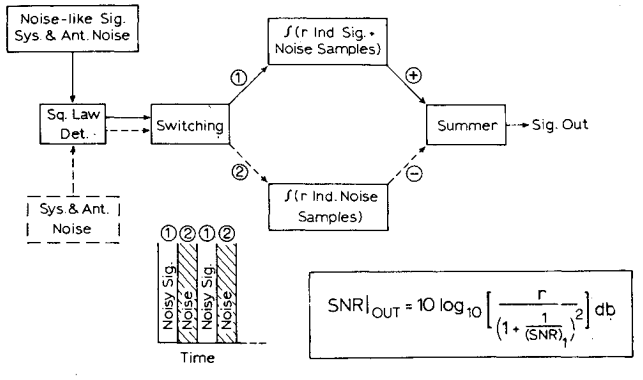

Fig. 6 S/N enhancement scheme for noise-like signals.

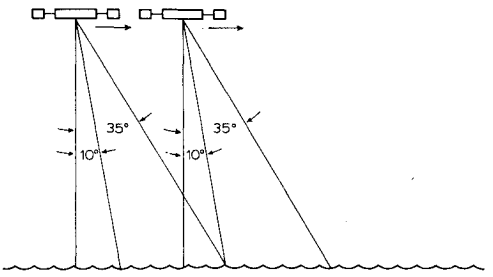

Fig. 7 Satellite-mounted scatterometer for sea state measurements.

radiometer calibration. If transmitter feedthrough is small enough, the first and last operations can go on simultaneously; otherwise a separate time interval is required for each. At the end of this cycle, the transmitter operates once more, and the entire cycle repeats. At longer intervals the radiometer is further calibrated by connecting the input to a cold reference source.

An along-track RADSCAT system could be built that would perform exactly the measurements indicated for Figs. 1–3. As illustrated in Fig. 7, measurements would be made at two angles (e.g., 10° and 35°) with either a dual-beam antenna or a two-step scanned antenna. Each pass of the satellite provides data only along the subsatellite track. Observations to date indicate such a system operating at 2.25 cm can make the required windspeed determinations. Perhaps some other wavelength would be better, but data are not available to verify it.

A more appropriate system proposed for operational use scans from side to side about the subsatellite track for a total swath of about 1200 km. By making observations every 120 km across this scan, a series of 11 tracks of observations will be made available for each pass of the satellite if the scan is ±600 km. Such a system depends on the assumption that absolute measurements at individual angles can be used to determine windspeed, so that normalization is unnecessary.

The proposed scanning system is illustrated in Fig. 8. The antenna is tilted forward by an angle β such that return at the minimum incidence angle is relatively sensitive to windspeed. Ideally such a system would use a scanner designed to produce a constant angle of incidence and polarization for all illuminated areas, but this would be much more difficult to build than the simple linear scanner illustrated.

Figure 9 shows the range of incident angles encountered for a satellite at 1000-km altitude with different tilt angles. The minimum angle of incidence is greater than the tilt angle because of the curvature of the earth. Because the maximum incident angle is not very sensitive to tilt angle, β can be 20° or even 25° without making the maximum angle of incidence much larger than for a tilt angle of 15°; and the larger tilt angle will permit more sensitivity to windspeed along the ground track. Too large a maximum incident angle would result in a scattering coefficient so small that more transmitter power would be needed.

With the proposed system, the contemplated circular beam width is about 20 mr. The observed ground spot is elliptical in shape because of tilt. Because scanning is in one direction only, the antenna may consist of a set of linear arrays, with only the phase between the linear arrays being adjusted electronically. An equal-incident-angle scanner would require adjusting the phase within, as well as between, linear arrays.

Analysis of Data to Be Obtained by the Satellite Instrument

The proposed RADSCAT instrument will provide data on a checkerboard grid of points about 600 km each side of the

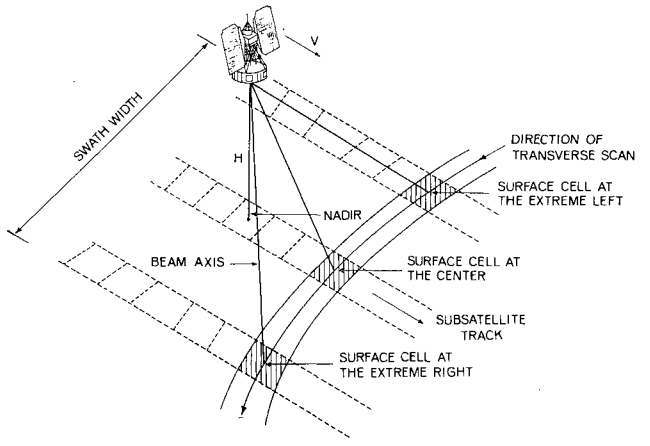

Fig. 8 Satellite-mounted scatterometer for sea state measurements—cross track scan.

subsatellite track to give essentially global coverage twice a day. The radar scattering cross section data are given by

$$\sigma^\circ = \sigma^\circ(\theta, |\mathbf{V}|, \chi)$$

with θ the angle of incidence, $|\mathbf{V}|$ the windspeed, and χ the wind direction. The incidence angle θ is known from the conditions of the measurement, but both of the other variables are to be determined from this measurement and other data. The effect of direction χ is considerably weaker than the effect of windspeed at 2.25-cm wavelength. Hence, if σ° and θ are known, the possible values of $|\mathbf{V}|$ could range about a central value $|\mathbf{V}|^*$ plus or minus four or five knots as χ varies through 360°. If both θ and χ are known, the value of windspeed can be inferred from σ° with considerably better accuracy, at least for winds up to 49 knots.

Additional complications may occur if σ° is dependent on properties of the waves not due to the current local wind, but this appears unlikely, at least for high windspeeds. At lower winds, surface roughness caused by mixing of wave trains arriving from different directions may contribute significantly to the observations, in which case the forecasting programs can be changed to take this effect into account. Gathering data to check this point will be easier for an instrument in space than for one on an aircraft, for a wide variety of these conditions must be located and the aircraft flown to them—a difficult task.

Data Obtained

The proposed instrument will yield about 40,000 pairs of numbers $\sigma^\circ(\theta, |\mathbf{V}|, \chi)$ and $T_e(\theta, \chi)$, simultaneously observed at known instants of time by the spacecraft. Some small subset of these pairs will be rejected because of high values of T_e and the presence of sea ice. The remaining values of $\sigma^\circ(\theta, V, \chi)$ can then, from knowledge of the orbit, be ordered as a five-dimensional vector of the form

$$\sigma^\circ_1(\theta, |V|, \chi), \quad \theta_1, \quad \lambda_1, \quad \phi_1, \quad t_1$$
$$\sigma^\circ_2(\theta, |V|, \chi), \quad \theta_2, \quad \lambda_2, \quad \phi_2, \quad t_2$$
$$\vdots$$
$$\sigma^\circ_{35,000}(\theta, |V|, \chi), \quad \theta_{35,000}, \quad \lambda_{35,000}, \quad \phi_{35,000}, \quad t_{35,000}$$

where λ and ϕ are longitude and latitude.

For $\sigma^\circ(\theta, V, \chi)$ given to the nearest tenth of a db, θ, λ, and ϕ given to the nearest 10th of a degree, and time to the nearest second, σ° contains about 10 bits, θ; 10 bits, the longitude and latitude 14 and 12 bits, respectively; and time 16 bits so that one vector is described by about 52 bits. If 35,000 measurements are used, the result is about 2.2 megabits/day of which only 350,000 bits plus time need to be transmitted by the spacecraft and the rest are derivable from orbit considerations. A data rate, even exaggerated, of 2.2 megabits/day is low compared to the data rates needed to transmit and receive television images. This volume of data can be easily processed on a modern computer.

Other Available Data

Other data are also available from the conventional meteorological sources and from spacecraft. Conventional data are from ground-based weather stations, radiosonde ascents over islands and continents, and ship reports. Other spacecraft data are cloud television images in the visible and infrared and the recent NIMBUS data equivalent to radiosonde ascents over the ocean.[18,19]

These data are not sufficiently dense to provide the resolution and accuracy needed to describe correctly the initial state of the atmosphere for numerical weather prediction purposes. In particular, from the observational point of view, the lowest layer of the atmosphere over the oceans is one of the most poorly defined parts of this initial value problem. From the theoretical point of view, much has been learned that could be put to practical use as shown by the text of Phillips[20] and a recent symposium on boundary layers and turbulence.[21]

The quality of the meteorological analyses over the ocean degrades progressively on going from the North Atlantic to the North Pacific, to the Indian Ocean, and, finally, to the Southern Hemisphere oceans, where data at the ocean surface and for the atmosphere over the ocean are extremely scarce.

The latest success of the NIMBUS program is an instrument that provides the equivalent of a meteorological sounding through clear skies. These data are presently being incorporated into numerical weather prediction methods, as described by Smith and Woolf.[19] It would be very helpful if the atmospheric pressure at the ocean's surface and the winds in the planetary boundary layer could be better specified for these same numerical weather prediction models.

Our knowledge of the planetary boundary layer over the oceans is based mainly on information radioed to central collection sites by ships at sea every six hours at 0000, 0600, 1200, and 1800 Greenwich Mean Time. These ships observe the windspeed and direction representative of conditions about 20 m above the sea surface. They also report air temperature, dew point, sea temperature, surface pressure, and other meteorological parameters.

The difficulty is that there are not enough ships sending back these data so that there are large gaps in the coverage.

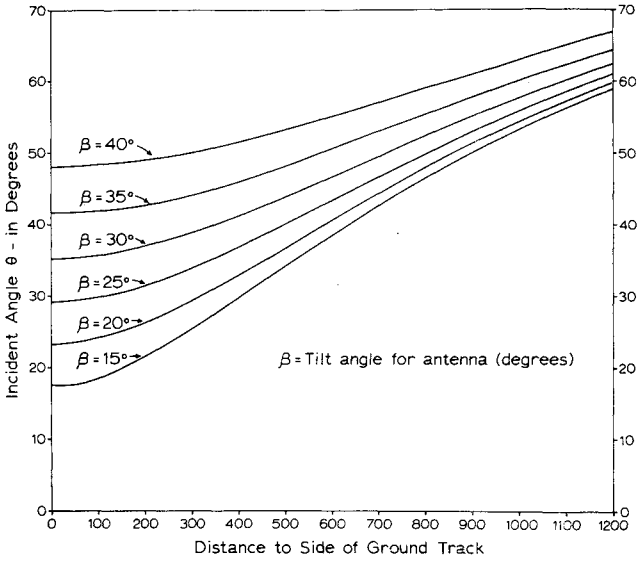

Fig. 9 Incident angle at the earth for a wave from a scanning antenna on a 1000-km altitude satellite (distance in km).

Ships avoid the areas of the oceans with the strongest winds, and probably, even now, the meteorological analyses are being degraded by this effect. The result is that the analysis of the conditions near the surface of the oceans has to be based on extensive interpolations of the available data, which produce errors in the initial value spacification used in the numerical prediction models.

Extensive studies of the effects of these errors, caused by poor coverage and erroneous reports in initial value specification, on northern hemisphere meteorological predictions have been made. The errors approximately double in importance each day so that after four days they magnify by about sixteen times. The four-day forecasts produced by numerical prediction models are not very good at the present time, in part for this reason. In a description of the present NOAA numerical prediction model, Shuman and Hovermale[22] showed several examples where three-day forecasts apparently failed because of erroneous initial value specifications over either the North Atlantic or the North Pacific Oceans.

The data provided by the RADSCAT can be used to upgrade the accuracy of the initial value specifications over the surface of the oceans to such an extent that significantly improved meteorological predictions in the two-, three-, and four-day time frame will be produced. The purpose of our present research and development effort is to have the computer programs and analysis techniques ready for use operationally by the time the instrument is flown on a spacecraft. After a brief two-month checkout of the data and the procedures, the data from the spacecraft can be incorporated into the then available numerical meteorological model and used on a real-time basis for meteorological predictions.

Present work consists of developing the computer programs for a model of the system that will prove even before the spacecraft flies that the procedure will be of value. These same programs will be capable of using the actual data that would be obtained by the system.

These same programs can serve as an input to numerical wave specification and prediction procedures as described in a series of reports by Pierson, Tick, and Baer[23]; Inoue[24]; and Bunting.[25] Should, for example, radar sea return depend to some extent on the longer waves in a wave spectrum, these methods will permit such effects to be taken into account.

Planetary Boundary Layer over the Oceans

The winds over the ocean are turbulent, and the goal for numerical weather prediction and for wave prediction is to determine the average wind (as averaged over about 20 min) over a grid of points as a function of elevation above the ocean surface from the surface to an elevation of about 1000 m. The windspeed and direction varies with height above the ocean surface, and thus the windspeed and direction reported by a ship at sea depends on the elevation of the anemometer above the surface, if the ship uses an anemometer, and on the training of an observer if the winds are estimated instead of measured.

Moreover, the variation of the wind with elevation immediately above the sea surface depends on the stability of the atmosphere. If the lapse rate is adiabatic, the logarithmic law is obeyed, but if the lapse rate is either stable or unstable, the departure of the wind from logarithmic can be substantial. The Keyps equation has to be used to describe these variations of the wind with height. (See, for example, Lumley and Panofsky,[26] pp. 111–114.)

To describe the structure of the winds in the planetary boundary layer, Cardone[27] has shown that it is necessary to consider the thermal structure of the boundary layer between the surface and the gradient wind level and that special care is required for the first 100 m or so above the surface.

Seven different quantities, some of them vectors, need to be determined as a field of values over the grid used. They are: $U_+ = (\tau/\rho)^{1/2}$, the friction velocity; a = the inflow angle across the isobars that determine the direction of U_+; Ri = the Richardson number used in the Keyps formulas; $\mathbf{V}_{19.5}$ = the wind at 19.5 m, used in wave forecasting; $\mathbf{V}_g$ = the gradient wind above the friction layer; $\mathbf{V}_t$ = the thermal wind between the surface and the gradient wind level; and p = the atmospheric pressure at the ocean surface.

Cardone's[27] analysis of the specification of the planetary boundary layer demonstrates ways to obtain these quantities on a grid with four times the number of points used in the conventional NWP grid. Only conventional ship reports are used. However, since past data are used, the many ship reports sent in several months later by mail can also be a part of the data bank for climatological purposes. This analysis procedure will be tested further and used to generate a wave climatology for the North Pacific. It will also provide high-quality analyses of the winds over the oceans to be used in simulating the data that would be obtained by the proposed instrument.

Use of Spacecraft Data

A NIMBUS spacecraft with a declination of 100° (a retrograde orbit), orbits the earth about 13 times in 24 hr with an orbital period of about 111 min. Successive northbound, or southbound, passes move about 27° westward each orbit and occur at either local noon or local midnight at the equator. The subsatellite track reaches to 80° North and South. Small lens-shaped voids in data coverage occur, but in polar latitudes the same portion of the ocean may be viewed with different values of θ and χ on several successive passes. A typical data density, worked out for an earlier geometry of the instrument, is shown in Fig. 10 for the northern and southern hemispheres. The very great density of coverage in the polar latitudes is important because these are the areas of strong winds and poor conventional data.

Between two successive synoptic reporting times, a NIMBUS spacecraft will survey about one-half of the earth (two opposing 90° sectors, one in daylight and one at night). A problem is to simulate the data that would be obtained during such a time interval and show how it would be used to improve the analysis in the planetary boundary layer.

This simulation is presently under development at New York University by L. Druyan. As a first step, the nonsynopticity of the spacecraft data will not be treated. The analyses obtained by Cardone[27] and the equations for the values of $\sigma^\circ(\mu, |\mathbf{V}|, \chi)$ will be used to generate a grid of data such as that which would be obtained for a radar for the Pacific Ocean. The analysis based on the very dense coverage made possible by using all available conventional data will be considered to be the true analysis from which the true values of σ° can be derived.

Then the true analysis will be degraded by deleting various percentages of the available ship reports. For example, about half of the available ship reports are not transmitted by radio and are not collected in time to be used in weather prediction. Where ship reports are deleted, errors in the pressure field, such as those that would occur from interpolating over larger distances, will be introduced. The differences in the winds and pressures obtained by an analysis of degraded fields and the true fields will provide a measure of the quality of present-day meteorological initial value inputs.

Then, finally, the computed values of $\sigma^\circ(\theta, \mathbf{V}, \chi)$ will be used to correct the degraded fields and to find out how closely the original true fields can be reconstructed. The percentage improvement over the degraded field will be a measure of the value of the radar data. Moreover, for those areas of the ocean where even the true data were based on inadequate coverage, the percentage improvement might even be expected to apply, given actual RADSCAT data.

The number of ship reports available for a given synoptic analysis is much greater at 0000Z and at 1200Z than at 0600Z

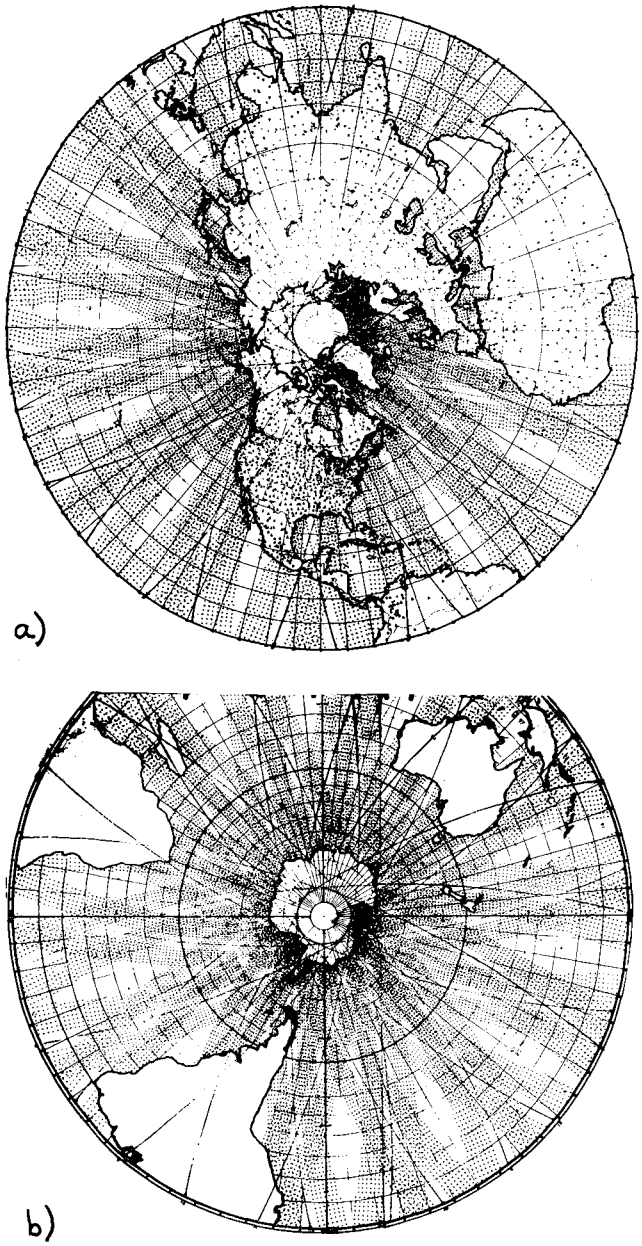

Fig. 10 a) Coverage for the northern hemisphere during 24 hr. b) Coverage for the southern hemisphere during 24 hr.

and 1800Z. The true data for a 0000Z analysis can then be degraded even further to simulate an 0600Z analysis. Even further, the Northern Pacific can be used to simulate the South Pacific by deleting even more ships and degrading the analysis still more since the conventional data coverage in the southern hemisphere is very poor indeed.

Bristor, Callicott, and Bradford[28] have developed a computer program that takes NOAA satellite images and produces polar stereographic cloud charts for each hemisphere as well as an equatorial Mercator projection cloud chart. Because they permit the location of fronts and low centers over the oceans, these cloud maps have proved extremely valuable in preparing the analysis of the surface charts for the southern hemisphere. With the quadrupled resolution used in the numerical techniques under development, the cloud images can be used to locate wind shear lines at fronts and the centers of lows where ship reports are absent.

The programs that will employ the radar data will also permit the use of cloud imagery to locate low centers and fronts and the use of NIMBUS sounding data to specify atmospheric stability, as well as all conventional surface reports.

Druyan has already developed portions of the program that will be ultimately employed to accomplish these objectives. A few scattered conventional observations are needed. Given the location of a low center from cloud images, a few isolated ship reports, and simulated windspeeds only on a grid of points, it is now possible to reconstruct a realistic surface pressure field that correctly locates the low center and gives the wind directions (which were originally known only at the ships).

The next step will be to simulate $\sigma^\circ(\theta, |\mathbf{V}|, \chi)$ values on a grid but use only the σ° and θ values. A first-guess wind field will define tentative χ, $|\mathbf{V}|$ fields which can then be iterated to produce a corrected wind and pressure field that would reproduce the original $\sigma^\circ(\theta, |\mathbf{V}|, \chi)$ field.

A very preliminary example of the kind of analysis that can result is illustrated in Figs. 11 and 12. The first shows a portion of the South Atlantic Ocean along the Greenwich Meridian. The dots represent the locations of the surface reports that were used in preparing the analysis of the surface pressure field that is shown. The high has a central isobar of 1024 mbars, for example, and the low on the lower left has a central isobar of 968 mbars. The analysis of this vast area (about 25 million square kilometers) is based on 21 surface weather reports and on NOAA cloud images, which located the low center south of Africa. It was not possible to analyze the pressure field for this low.

Figure 12 shows schematically the data that would be obtained from the proposed instrument in about 27 min for one quarter of one orbit. The σ° values have been assumed to have been converted to windspeeds. There are over one thousand values plotted for the winds over the ocean surface. They are, of course, completely fictional since the instrumented spacecraft does not exist. However, the revised analysis that could result for such data show substantial changes between this and the preceding figure. In particular, the low south of Africa is much better defined since winds of 35 knots were hypothetically detected on its edge.

Preceding and subsequent spacecraft passes over this oceanic area would provide data on the winds at roughtly two-hour intervals, and virtually complete, and often overlapping, coverage from 35°S to the continent of Antarctica. It is clear that this proposed instrument will be of immense value in defining accurately the winds over the oceans of the southern hemisphere.

Nonsynopticity of Satellite Data

One of the basic problems in combining satellite data and conventional data is that the satellite data are continuous with time so that only a few observations are actually taken within, say, ±20 min of the synoptic observing times. The cloud images in Fig. 11b are really a spacetime plot throughout one day where adjacent strips differ by about 111 min, and there is a 24-hr time discontinuity somewhere on each map. The cloud and spacecraft data should really be thought of as being plotted in cylindrical coordinates on a helical surface with time as the vertical axis.

A second problem is thus to relate all past spacecraft data with a cut-off time of about one hour after synoptic map time to a given synoptic chart so as to improve its analysis. If data available up to, say, 1300 Greenwich are to be analyzed so as to improve the 1200 Greenwich chart, this implies both forward and backward extrapolations and interpolations in time so as to get the best analysis.

Here some fairly sophisticated procedures will be needed. Present numerical methods actually generate a predicted surface field every ten mintues or so in order to produce two,-three-, and four-day predictions. The set of the most recently prepared fields, i.e., the forecasted fields for the past six hours produced by the most recent initial value data, could be used

to predict what the spacecraft should have observed in orbit. The discrepancy between observed and predicted values could then be used to correct the predictions.

For the synoptic map time under analysis, the prediction model will then have evolved to that planetary boundary-layer model that can be made most consistent with all past radar and conventional data and the present set of synoptic data.

Also, the two most recent orbits of the spacecraft will have viewed some fairly large region of the ocean twice at times straddling the synoptic map time. A simple interpolation under these conditions will provide a field of windspeeds to be used directly in a given synoptic analysis.

Conclusion

A system using a satellite-borne radar-radiometer for obtaining predictions of surface winds and waves over the surface of the world's oceans has been described. The radar permits windspeed determination, and the radiometer permits correction for attenuation in the atmosphere. The radiometer also should give useful information on the world-wide distribution of precipitation.

Methods have been indicated whereby this kind of data can be integrated with other types of observations to provide the required wind direction needed to interpret these data, and at the same time to use these data to greatly improve oceanic weather and wave forecasting, particularly in the southern hemisphere.

The observed radar returns definitely indicate that an along-track 2.25-cm system is feasible, but taking full advantage of the satellite platform requires a scanning system to increase the swath from which data are obtained. That such a system will be successful can be inferred from combination of observation with theory, but confirmation will require additional measurements with better control of absolute calibration.

The proposed system uses the same receiver for both radar and radiometer, and a time-sharing scheme between radar transmission (ICW), radar and radiometer reception, and radiometer calibration. When this technique is used, a 1-m square antenna permits a radar average power of less than 5 w and a total system power and weight well within the capability of the NIMBUS series of satellites.[16]

Future Meteorological Observations Systems and Weather Prediction Systems

The use of spacecraft to obtain data for true prediction purposes for both meteorology and oceanography is in its infancy. Cloud images are extremely useful, but at present they are employed in a qualitative way. The new sounding techniques [SIRS] provide the first quantitative data for numerical prediction purposes. The instrument we propose would provide a second source of global quantitative data measured by a spacecraft. A combination of the two, plus conventional data, could conceivably make it possible to do numerical weather predictions on a global, instead of northern hemisphere, basis and thus eliminate one of the great difficulties that will be encountered in trying to extend the accuracy of meteorological predictions beyond five or six days. Air movements across the equator from one hemisphere to the other become important at these forecast ranges, especially during the northern hemisphere winters. It is possible to imagine three NIMBUS-type spacecraft separated by 120° such that complete coverage for clouds, infrared, and albedo measurements, atmospheric soundings and radar measurements would be obtained over the globe in four hours. The data rates for the soundings and the radar measurements are well within the present abilities to process the data, and the result would be, as the numerical prediction models be-

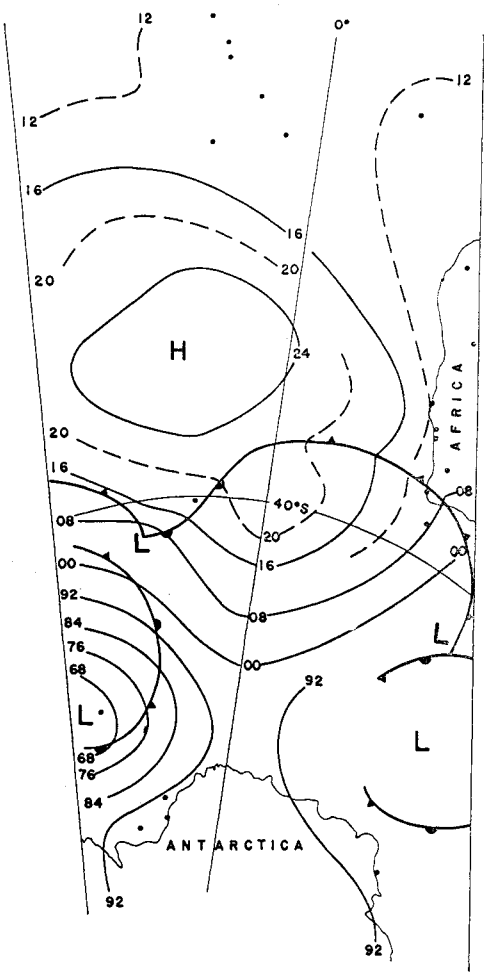

Fig. 11a Portion of the National Meteorological Center Southern Hemisphere surface analysis for Jan. 18, 1968. The dots represent points where surface reports were available for the analysis. The analysis is based on these surface points, the southern hemisphere cloud mosaic patterns prepared by NOAA, and continuity considerations.

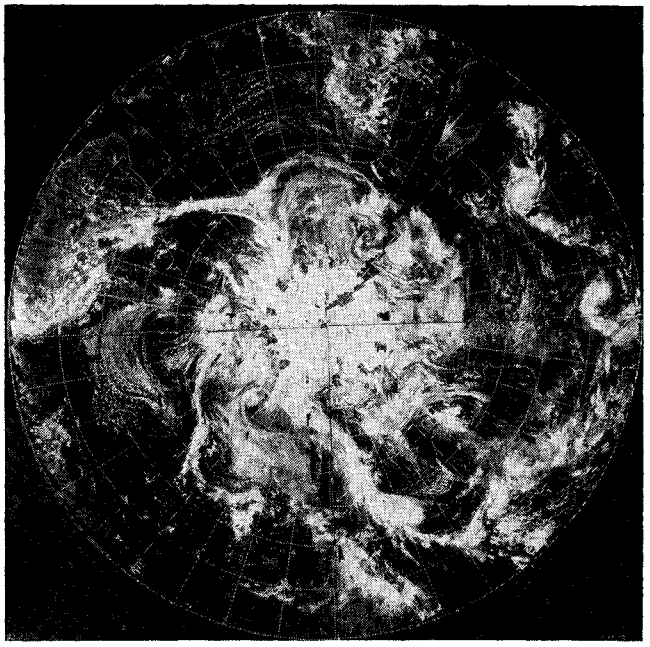

Fig. 11b The corresponding cloud photograph mosaic for Jan. 18, 1968. Note that the cloud pattern south of Africa is the reason for the low center on the surface analysis because of poor conventional surface data coverage.

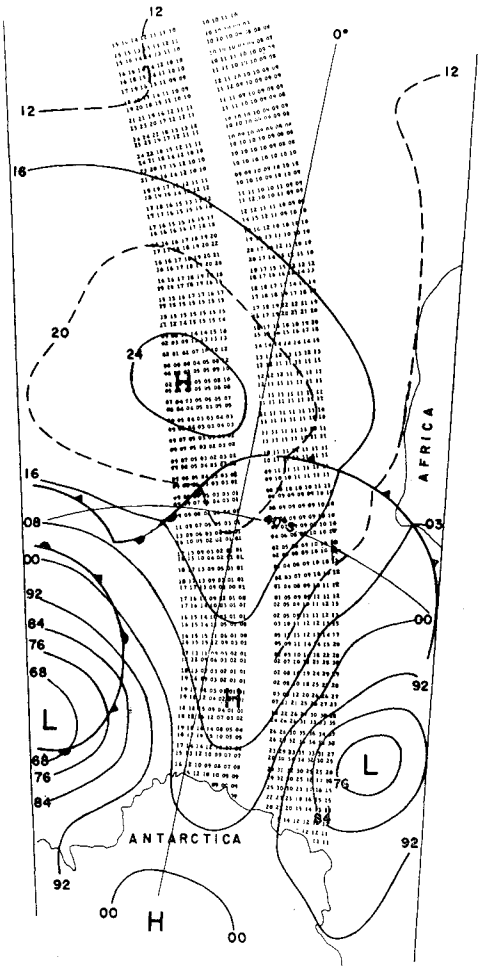

Fig. 12 Hypothetical data that might be obtained from one portion of one pass of a NIMBUS spacecraft with a scatterometer and dual antenna system. The numbers represent the windspeed in knots on a grid that approximates the actual coverage.

come more refined,[29] extremely valuable predictions of the weather for as much as five or six days into the future.‡

References

[1] Beckmann, P. and Spizzichino, A., *The Scattering of Electromagnetic Waves from Rough Surfaces*, Macmillan, New York, 1963.

[2] Skolnik, M., "A review of Radar Sea Echo," Rept. 2025, July 1969, U.S. Naval Research Lab., Washington, D.C.

[3] Moore, R. K. and Bradley, G. A., "Radar and Oceanography," *Proceedings of the 1969 Earth Resources Review*, NASA/MSC, Houston, Sept. 1969.

[4] Guinard, N. W. and Daley, J. C., "An Experimental Study of a Sea Clutter Model," *Transactions of the IEEE*, Vol. 58, No. 4, 1970, pp. 543–550.

[5] Wright, J. W., "A New Model for Sea Clutter," *Transactions of the IEEE*, Vol. AP-16, 1968, pp. 217–223.

[6] Bass, F. G. et al., "Very High Frequency Radioactive Scattering by a Disturbed Sea Surface," *Transactions of the IEEE*, Vol. AP-16, 1968, pp. 554–568.

[7] Fung, A. K. and Chan, H. L., "Backscattering of Waves by Composite Rough Surfaces," *Transactions of the IEEE*, Vol. AP-17, 1969, pp. 590–597.

[8] Kerr, D. E., *Propagation of Short Radio Waves*, McGraw-Hill, New York, 1951.

[9] Stogryn, A., "The Apparent Temperature of the Sea at Microwave Frequencies," *IRE Transactions: Antennas and Propagation*, Vol. AP-15, March 1967, pp. 278–286.

[10] Nordberg, W., private communication, 1969, Goddard Space Flight Center, Greenbelt, Md.; also Nordberg, W. et al., "Measurements of Microwave Emissions from a Foam Covered Wind Driven Sea," to be published in *Journal of Atmospheric Sciences*.

[11] Williams, G. F., "Microwave Radiometry of the Ocean and the Possibility of Marine Wind Velocity Determination from Satellite Observations," *Journal of Geophysical Research*, Vol. 74, No. 18, Aug. 1969, pp. 4591–4594.

[12] Kreiss, W. T., "The Influence of Clouds on Microwave Brightness Temperature Viewing Downward over Open Seas," *Proceedings of the IEEE*, Vol. 57, No. 4, April 1969, pp. 440–445.

[13] Singer, S. F. and Williams, G. F., "Microwave Detection of Precipitation over the Surface of the Ocean," *Journal of Geophysical Research*, Vol. 77, No. 10, May 1968, pp. 3324–3327.

[14] Wilson, R. W., "Sun-tracker Measurements of Attentuation by Rain at 16 and 30 GHz," *Bell System Technical Journal*, Vol. 48, 1969, pp. 1383–1404.

[15] Rouse, J. W., "Arctic Ice Type Identification by Radar," *Proceedings of the IEEE*, Vol. 57, 1969, pp. 605–611.

[16] Moore, R. K. and Ulaby, P. T., "The Radar Radiometer," *Proceedings of the IEEE*, Vol. 57, 1969, pp. 587–590.

[17] Dicke, R. H., "The Measurement of Thermal Radiation at Microwave Frequencies," *Review of Scientific Instrument*, Vol. 17, 1946, pp. 268–275.

[18] Wark, D. Q., Fleming, H. E., and Hilleary, D. T., "Measurements of Atmospheric Temperature Profiles with the Satellite Infrared Spectrometer," (abstract only), *E⊕S Transactions of the American Geophysical Union*, Vol. 50, No. 11, 1969, p. 622.

[19] Smith, W. L. and Woolf, W. M., "Synoptic Analysis of Satellite-Borne Temperature Profile Observations," (abstract only), *E⊕S Transactions of the American Geophysical Union*, Vol. 50, No. 11, 1969, p. 122.

[20] Phillips, O. M., *The Dynamics of the Upper Ocean*, Cambridge University Press, 1966.

[21] Bowden, K. R., Frenkiel, F. N., and Tani, I., *The Physics of Fluids Supplement*, IUGG and IUTAM Symposium on Boundary Layers and Turbulence, American Institute of Physics, 1967.

[22] Shuman, F. C. and Hovermale, J. B., "An Operational Six Layer Primitive Equation Model," *Journal of Applied Meteorology*, Vol. 7, No. 9, pp. 525–547.

[23] Pierson, W. J., Tick, L. J., and Baer, L., "Computer Based Procedures for Preparing Global Wave Forecasts and Wind Field Analyses Capable of Using Wave Data Obtained by a Spacecraft," ACR-136, 1966, Sixth Symposium Naval Hydrodynamics, Office of Naval Research, Dept. of the Navy.

[24] Inoue, T., "On the Growth of the Spectrum of a Wind Generated Sea According to a Modified Miles-Phillips Mechanism and its Application to Wave Forecasting," TR-67-5, 1967, Geophysical Sciences Lab., New York U., Bronx, N.Y.

[25] Bunting, D., "Evaluating Ocean Wave Spectra Forecast," *Journal of Geophysical Research*, Vol. 75, No. 21, pp. 4131–4143.

[26] Lumley, J. L. and Panofsky, H. A., *The Structure of Atmospheric Turbulence*, Interscience Publishers, New York, 1964.

[27] Cardone, V., "Specification of the Wind Distribution in the Marine Boundary Layer for Wave Forecasting," TR-69-1, 1969, Geophysical Sciences Lab., New York U., Bronx, N.Y.

[28] Bristor, C. L., Callicott, W. M., and Bradford, R. D., "Operational Processing of Satellite Cloud Pictures by Computer," *Monthly Weather Review*, Vol. 94, No. 8, Aug. 1966, pp. 515–527.

[29] Smagorinsky J., Wexler Memorial Lecture, National Meeting of American Meteorological Society, Jan. 1969.

[30] Naugle, J. E., "Opportunities for Participation in Space Flight Investigations," Memo Change 33, Dec. 22, 1970, NASA.

‡ Note added in proof: An instrument that has many of the features of the radar-radiometer described in this paper, and that will also be a radar altimeter, is to be flown on a manned spacecraft (Skylab) as described in an "Opportunities" document issued by NASA.[30] This instrument (S193) is much more sophisticated than the one described herein and will provide voluminous data for the final design of an instrument to meet the objectives described in this paper.